This article has been accepted for publication in a future issue of this journal, but has not been fully edited. Content may change prior to final publication. Citation information: DOI 10.1109/TSG.2017.2777789, IEEE Transactions on Smart Grid

A Comprehensive Model to Integrate Emerging Resources from Supply and Demand Sides

Miadreza Shafie-khah, *Senior Member, IEEE,* Nadali Mahmoudi, *Member, IEEE,* Pierluigi Siano, *Senior Member, IEEE,* Tapan K. Saha, *Senior Member, IEEE,* and João P. S. Catalão, *Senior Member, IEEE*

***Abstract*—This paper extensively models the interactions of emerging players in future power systems to analyze their impacts on electricity markets. To this end, renewable energy resources are modeled in such a way that wind power poses uncertainty on the supply side, and rooftop photovoltaics (PVs) add uncertainty to the demand side. Moreover, both uncontrolled and controlled behaviors of individual electric vehicles (EV) in electricity markets are addressed through a new EV model. Further, a comprehensive demand response (DR) model considering several customer-driven constraints is developed to undertake the practical constraints of customers. A stochastic market clearing formulation is presented to comprehensively account for the unique features of the given resources while evaluating their impacts. The numerical results clearly show the importance of such modeling in electricity markets to investigate the mutual impacts of emerging resources.**

***Index Terms*—Demand response, electric vehicle, emerging resources interaction, wind power, rooftop PV.**

NOMENCLATURE

A. Indices (Sets/Size)

b (B)	Network bus
dra (DRA)	DR aggregators
eva (EVA)	EV aggregators
i (I)	Conventional units
j (J)	Loads
l (L)	Lines
$lc\,(LC)$, $lg\,(LG)$, $lrc\,(LRC)$, $ls\,(LS)$	Load curtailment, growth, recovery, and shifting programs
n (N)	EVs
p (P)	DR programs
t (T)	Time periods
ω (Ω)	Scenarios
wpp (WPP)	Wind power units
x	Market players dra, eva, i, and wpp

J.P.S. Catalão acknowledges the support by FEDER funds through COMPETE 2020 and by Portuguese funds through FCT, under Projects FCOMP-01-0124-FEDER-020282 (Ref. PTDC/EEA-EEL/118519/2010), POCI-01-0145-FEDER-016434, POCI-01-0145-FEDER-006961, UID/EEA/50014/2013, UID/CEC/50021/2013, and UID/EMS/00151/2013, and also funding from the EU 7th Framework Programme FP7/2007-2013 under GA no. 309048.

M. Shafie-khah is with C-MAST, University of Beira Interior, Covilhã 6201-001, Portugal (miadreza@ubi.pt).

N. Mahmoudi and T. K. Saha are with the University of Queensland, Brisbane, Australia (n.mahmoudi@uq.edu.au, saha@itee.uq.edu.au).

P. Siano is with the University of Salerno, Salerno, Italy (psiano@unisa.it).

J.P.S. Catalão is with INESC TEC and the Faculty of Engineering of the University of Porto, Porto 4200-465, Portugal, also with C-MAST, University of Beira Interior, Covilhã 6201-001, and also with INESC-ID, Instituto Superior Técnico, University of Lisbon, 1049-001, (e-mail: catalao@ubi.pt).

B. Parameters

C_{wpp}^{sp}	Cost of wind spillage of wind power unit wpp
$Cap_{n,\omega}^{\mathrm{EV}}$	Capacity of EV n in scenario ω
$D_{dra,p}^{\max}$	Maximum ON time of DR program p by DR aggregator dra
$D_{dra,p}^{\min}$	Minimum ON time of DR program p by DR aggregator dra
$E_{dra,p}$	Max energy which can be provided by DR program p of DR aggregator dra
$F_l^{\max}$	Transmission line flow limit of line l
$F_{dra,p,t}^{\max}$	Max available DR volume by DR program p of DR aggregator dra in time period t
$L_{j,\omega,t}^{\mathrm{N}}$	Net load j in in scenario ω and time period t
$N_{dra,p}$	Maximum number of DR program p by DR aggregator dra
$N_{eva,\omega,t}$	Number of EVs of EV aggregator eva in scenario ω and time period t
NG	Number of conventional units
$P_{wpp,\omega,t}^{\mathrm{Act}}$	Power production of wind power unit wpp in scenario ω and time period t
$P_{wpp}^{\max}$	Maximum capacity of wind power unit wpp
$P_i^{\max}$	Maximum capacity of conventional unit i
P_i^{SD} P_i^{SU}	Startup and shut down limits of conventional unit i
$RCF_{dra,ls/lrc}$	Recovery factor of load recovery programs by DR aggregator dra
RD_{dra}^{DR} RU_{dra}^{DR}	Maximum reserve up and down capacity by DR aggregator dra
RD_x, RU_x	Ramp-down and -up limits of player x
$roc_{dra,p,t}$	Maximum rate of change of DR program p by DR aggregator dra between two consecutive periods
$soc_n^{\min}$, $soc_n^{\max}$	Minimum and maximum state of charge levels of EV n
$soc_n^{\mathrm{EV,ini}}$	Initial state of charge of EV n at the level of scenario generation
$soc_{n,\omega,t}^{\mathrm{EV,ini}}$	Initial state of charge of EV n in scenario ω and time period t
$soc_n^{\mathrm{EV,ds}}$	Desired state of charge of EV n at the departure time
$soe_{eva,\omega,t}^{\mathrm{arv}}$	State of energy of arrived EVs in scenario ω and time period t
SUC_i	Start-up cost of conventional unit i
t_n^{arv}	Arrival time of EV n

This article has been accepted for publication in a future issue of this journal, but has not been fully edited. Content may change prior to final publication. Citation information: DOI 10.1109/TSG.2017.2777789, IEEE Transactions on Smart Grid

$t_n^{\text{arv,min}}$, $t_n^{\text{arv,max}}$	Minimum and maximum arrival time of EV n
t_n^{dep}	Departure time of EV n
$t_n^{\text{dep,min}}$, $t_n^{\text{dep,max}}$	Minimum and maximum departure time of EV n
$T_{dra,p,t}^{\text{On}}$	The period in which DR program p by DR aggregator dra is valid
T_i^{Off}, T_i^{On}	Minimum OFF and ON times of conventional unit i
$X_{i,t}^{\text{Off}}$, $X_{i,t}^{\text{On}}$	OFF and ON time duration of conventional unit i
X_l	Reactance of line l
$Voll_j$	Value of lost load of load j
γ_n^{ch}, γ_n^{dch}	Charging and discharging rates of EV n
$\eta_{eva}^{\text{ch}}, \eta_{eva}^{\text{dch}}$	Average of charge/discharge efficiency of EVs of EV aggregator eva
$\lambda_{x,t}^{\text{Cap,R-dn}}$	Offer capacity cost of down-reserve of player x in time period t
$\lambda_{x,t}^{\text{Cap,R-up}}$	Offer capacity cost of up-reserve of player x in time period t
$\lambda_{x,t}^{\text{En}}$	Offer cost of energy of player x in time period t
$\lambda_{x,t}^{\text{R-dn}}$, $\lambda_{x,t}^{\text{R-up}}$	Offer energy cost of down and up-reserve of player x in time period t
π_ω	Probability of scenario ω

C. Variables

First-Stage Decisions:

$C_{i,t}^{\text{SU}}$	Start-up cost of conventional unit i in time period t
$F_{l,t}$	Line flow of line l in time period t
$I_{i,t}$, $SD_{i,t}$	Binary variables indicating the start-up and shut-down status at the beginning of period t
$L_{j,t}^{\text{S}}$	Scheduled load j in time period t
$P_{x,t}^{\text{En}}$	Scheduled power of player x in time period t
$P_{eva,t}^{\text{En,EVA2G}}$	Injected power of EV aggregator eva back to the grid in time period t
$P_{eva,t}^{\text{En,G2EVA}}$	Injected power of the grid to EV aggregator eva in time period t
$P_{x,t}^{\text{R-dn}}$, $P_{x,t}^{\text{R-up}}$	Scheduled down and up-reserve of player x in time period t
$u_{i,t}$	Binary variable indicating the ON/OFF status in time period t
$\delta_{ls,t}$ $\delta_{lr,t}$	Voltage angles of sending and receivers buses in time period t

Second-Stage Decisions:

$F_{l,\omega,t}$	Line flow of line l in scenario ω and time period t
$F_{dra,p,\omega,t}$	DR volume by DR program p of DR aggregator dra in scenario ω and time period t
$I_{dra,p,t}$	Binary variable indicating if DR program p of DR aggregator dra in time period t is started
$L_{j,\omega}^{\text{net}}$	Net load (original load minus rooftop PV)
$L_{j,\omega,t}^{\text{Sh}}$	Load shedding of load j in scenario ω and time period t
$P_{wpp,\omega,t}^{\text{sp}}$	Wind power spillage of wind power unit wpp in scenario ω and time period t
$P_{x,\omega,t}^{\text{Dep,R-dn}}$	Deployed down-reserve of player x in scenario ω and time period t
$P_{n,\omega,t}^{\text{Dep,R-dn,EV}}$	Deployed down-reserve of EV n in scenario ω and time period t
$P_{x,\omega,t}^{\text{Dep,R-up}}$	Deployed up-reserve of player x in scenario ω and time period t
$P_{n,\omega,t}^{\text{Dep,R-up,EV}}$	Deployed up-reserve of EV n in scenario ω and time period t
$P_{eva,\omega,t}^{\text{En}}$	Transferred power between the grid and EV aggregator eva in scenario ω and time period t
$P_{eva,\omega,t}^{\text{En,G2EVA}}$	Injected power of the grid to EV aggregator eva in scenario ω and time period t
$P_{eva,\omega,t}^{\text{En,EVA2G}}$	Injected power of EV aggregator eva back to the grid in scenario ω and time period t
$P_{n,\omega,t}^{\text{En,EV2G}}$	Injected power of EV n back to the grid in scenario ω and time period t
$P_{n,\omega,t}^{\text{En,G2EV}}$	Injected power of the grid to EV n in scenario ω and time period t
$S_{dra,drp,t}$	Binary variable indicating if DR program p of DR aggregator dra in time period t is stopped
$soc_{n,\omega,t}^{\text{EV}}$	State of charge of EV n in scenario ω and time period t
$soc_{n,\omega,t}^{\text{EV,dep}}$	State of charge of departed EV n in scenario ω and time period t
$soe_{eva,\omega,t}^{\text{dep}}$	State of energy of departed EVs of EV aggregator eva in scenario ω and time period t
$soe_{eva,\omega,t}^{\text{EVA}}$	State of energy of EV aggregator eva in scenario ω and time period t
$U_{eva,\omega,t}^{\text{EVA2G}}$, $U_{eva,\omega,t}^{\text{G2EVA}}$	Binary variables indicating the vehicle-to-grid and grid-to-vehicle operation modes of EV aggregator eva in scenario ω and in time period t
$V_{dra,p,t}$	Binary variable indicating the on/off status of deployed DR program p of DR aggregator dra in time period t
$\delta_{ls,\omega,t}$ $\delta_{lr,\omega,t}$	Voltage angles of sending and receivers buses in scenario ω and in time period t

Note that $\forall$ (index) implies $\forall$ (index) $\in$ its associated set in this paper.

I. Introduction

A. Motivation and Aims

Future power systems have to deal with the challenges and benefits of a number of emerging technologies. Although wind power may decrease the emissions of power systems, its inherent variability and intermittency can limit the quantity that can be integrated into the system. This is true of solar PVs, and even worse for rooftop PVs since they add further uncertainty to the demand side, which is beyond the control of Independent System Operators (ISOs). Demand Response (DR) aggregators are also emerging in electricity markets. These players have to consider the technical constraints of various programs in

This article has been accepted for publication in a future issue of this journal, but has not been fully edited. Content may change prior to final publication. Citation information: DOI 10.1109/TSG.2017.2777789, IEEE Transactions on Smart Grid

markets to prevent overestimation of DR potential. Further, as uncontrolled electric vehicle (EV) charging would cause sharp peaks in demand, control and aggregation may help coordinate charging and enhance diffusion of EVs connected to the power system. This means that EV aggregators (EVAs) require detailed modeling of the behavior and uncertainty of EVs.

This paper aims at proposing a new model that integrates the above emerging resources into electricity markets, while comprehensively addressing the challenges associated with each resource. The problem is formulated as a stochastic market clearing problem, which considers the uncertainties of the given resources, as well as their unique attributes and constraints.

B. Literature Review and Contributions

Modelling wind on the supply side is extensively studied in the literature. The existing studies mainly consider problems such as market clearing [1], locational marginal price [2], uncertainty impacts [3], and strategic bidding [4] in the presence of wind power. The studies of large-scale PVs, however, mainly target their impact on distribution networks [5], while a few papers consider these resources in markets [6]. The existing studies, however, fail to address the uncertainty of the demand as a result of high integration of rooftop PVs. Nowadays, rooftop PV is emerging in some electricity markets such as in the Australian National Electricity Market (NEM) [7], which adds more uncertainty and variability to the demand. This indeed makes the traditional demand modeling no longer valid. The given models usually disregard the uncertainty faced by demand and thus consider a deterministic model for the demand side [8]. Those studies addressing demand uncertainty apply simple models such as normal probability density function [1] and Laplace distribution [9], while disregarding the impacts of uncertain rooftop PVs.

Further development on the demand side is the presence of DR aggregators. The research on how to procure DR from consumers outweighs that of how DR aggregators trade the aggregated DR in the wholesale market. Detailed DR programs such as individual DR programs [10], building energy management [11], heating and cooling systems control [12], various incentive-based DR [13], new and innovative tariff designs [14] are amongst the most popular DR programs applied to consumers. DR trading in electricity markets, mainly by DR aggregators, is also presented in some research [15-20]. For example, authors in [16] consider DR as blocks of offers in the market. The main drawback of these studies is that they mostly put their emphasis on how to trade DR in electricity markets, while little attention has been paid to the way this DR is procured. Authors in [20] model and evaluate residential demand response in electricity markets, while DR is not modeled in detail. A dynamic model is proposed in [21], where DR is used to facilitate renewable energy integration. Another DR model is presented in [22], which only constraints the energy limit of DR in electricity markets. A reasonably comprehensive DR model is presented in [23], where only constraints such as the duration of DR and the number of responses in a day are considered.

Moreover, EV integration from the system operator's viewpoint is addressed in the literature, while mostly model EVs as lumped resources and their behavior and uncertainties are not taken into account. The integration of EVs and residential loads is studied from a distribution system operator's viewpoint in [24] to mitigate the peak demand of the system. The model indeed uses a prediction model while the required target level of the state of charge (SOC) is not considered. Different EV management approaches are compared in [25], for day-ahead energy resource scheduling. Authors in [26] consider EVAs in power systems as a type of dispatchable DR and energy storage system, while disregarding the major uncertainties faced by EVs. In [27], the interactions of parking lots and energy and reserve markets are modeled, whereas EVs are modeled using a lumped pattern disregarding the impact of each EV behavior. Considering a lump pattern for EVs has a crucial drawback. Using the lump pattern does not ensure that the technical constraints of each individual EV is satisfied. In other words, the minimum and maximum state of charge (SOC), as well as the charging and discharging rates for each EV are not considered. In addition, the desired SOC of one EV owner can be different with another EV owner that cannot be considered in the lump pattern models. All in all, in order to satisfy the technical constraints of EVs, these vehicles should be modeled individually. In order to overcome the drawback, this paper models the EVs individually.

The abovementioned renewable and emerging resources would affect the energy and reserve markets. Individual and mutual impacts of these resources have been studied in the literature. For example, mutual models for wind with DR [4, 28], and wind with EVs [29, 30], are delivered. However, there is no comprehensive model in the literature, which simultaneously represents the integration of all the given resources.

It should be noted that incorporating EVs into models in which DR has been considered is always complicated, because EVs can be considered as a part of demand which can also respond to market price variations or incentives in DR events. Although there are some reports that addressed different structures for DR and EVs, to the best of the authors' knowledge, there is no report in the literature that incorporates both DR aggregator and EV aggregator into a comprehensive market model. This comprehensive model is vital as it reveals an interpretation of how ISOs can utilize the unique characteristics of these resources to manage both energy and reserve markets.

Considering the above review of the literature, the key contributions of this work are highlighted below.

1. This paper proposes a comprehensive formulation of an integrated model of a renewable-based electricity market integrating wind systems on the supply side and rooftop PV, DR aggregators and EV aggregators on the demand side, while proposing their practical models, as given in the following. The model is formulated as a stochastic market clearing problem, which considers the given resources' uncertainty, unique attributes and constraints. We extensively study the proposed model in the case study and highlight the importance of such comprehensive modeling.
2. With regards to the modeling rooftop PV on the demand side, the contribution of this paper over the existing studies is the modeling of rooftop PV uncertainty, accounted for as negative demand to be deducted from the original demand.
3. Another contribution of the proposed method consists of the modeling of DR and of the DR aggregator taking into

This article has been accepted for publication in a future issue of this journal, but has not been fully edited. Content may change prior to final publication. Citation information: DOI 10.1109/TSG.2017.2777789, IEEE Transactions on Smart Grid

account the constraints imposed by the consumers. Further, we present practical models for two DR programs, i.e. load recovery and load growth, which are ignored in the existing studies. This consideration is necessary in the renewable-based electricity markets, where these programs need to be properly modeled in order to better utilize renewable resources and in particular to avoid their spillage.

4. Another innovative contribution of this paper consists of new models integrating the behavior of each single EV with that of the EVAs' offer into the energy and reserve markets by considering the uncertainties of arrival time, departure time, types of EV batteries and arrival SOC. Further, the desired SOC agreed with the EV owners is also incorporated into the proposed model.

Compared to the most relevant references (i.e. [23], [27] and [31]), we further explain our contributions as follows.

The given model [23] is deterministic while no wind and PV systems are considered. Further, the DR aggregator is proposed in such a way that only load shifting and load curtailment programs are considered. The given programs consider some practical constraints of consumers, but do not model other practical constraints we model in our work. In addition, reference [23] does not model how load is recovered through load recovery programs. Instead, they consider the load recovery as a lumped volume which is recovered during the off-peak period. This undermines the potential of load recovery programs, particularly when integrating renewable resources such as wind systems.

In [27] and [31], the EV parking lot (in [27]) or the EV aggregator (in [31]) are studied from the viewpoint of the owner of parking lot or the aggregator rather than an ISO. It is obvious that the concerns of the system operators are totally different than an EV aggregator that is a profit entity. Therefore, the formulation (the objective function and the constraints) is entirely different.

Second, the given models do not consider the details of each EV that are considered in the current manuscript. In other words, in [27] and [31], EVs are modeled using a lumped pattern disregarding the impact of each EV owner's behavior. However, in the current model, the behavior of each single EV is modeled in relation to the EV aggregators' offers into the energy and reserve markets by considering the uncertainties of arrival time, departure time, types of EV batteries and arrival SOC. Further, the desired SOC agreed with the EV owners is also incorporated into the proposed model while it is not considered in [27] and [31].

Lastly, this study further improves our previous work [32] in that we develop a comprehensive model integrating wind, solar PV, DR and EVs, and also presents the models of their interactions with different case studies.

Note that the proposed model takes into account the current practice in existing electricity markets. Wind power producers usually participate in the energy market, which is the case for the Australian National Electricity Market (NEM), and the US markets [33]. Rooftop PV accounts for a high share of renewable energy in Australia [34], where it is taken into account as negative demand. DR aggregators participate in both energy and reserve markets in PJM [35]. EV aggregators are still in early stages, but it has been argued in existing studies that they can participate in both markets [36].

II. Proposed Comprehensive Model

A. Demand Response

Four major DR programs, i.e. load shifting, load recovery, load curtailment, and load growth, are mathematically modeled. Each DR program has technical limitations such as its minimum and maximum potentials, minimum and maximum durations, energy limit, maximum rate of change for one period to the next one, and the number of times that the DRA can call them on a day [32]. These constraints are modeled in the following terms.

$$0 \le F_{dra,p,\omega,t} \le F^{\max}_{dra,p,t} V_{dra,p,t} T^{On}_{dra,p,t} \qquad \forall dra,p,w,t \qquad (1)$$

$$V_{dra,p,t} - V_{dra,p,t-1} = I_{dra,p,t} - S_{dra,p,t} \qquad \forall dra,p,t \ge 2 \qquad (2)$$

$$I_{dra,p,t} + S_{dra,p,t} \le 1 \qquad \forall dra,p,t \qquad (3)$$

$$\sum_{k=t}^{t+D^{\min}_{dra,p}-1} V_{dra,p,k} \ge D^{\min}_{dra,p} I_{dra,p,k} \qquad \forall dra,p,k \qquad (4)$$

$$\sum_{k=t}^{t+D^{\max}_{dra,p}-1} S_{dra,p,k} \ge I_{dra,p,k} \qquad \forall dra,p,k \qquad (5)$$

$$-roc_{dra,p,t} \le F_{dra,p,\omega,t} - F_{dra,p,\omega,t-1} \le roc_{dra,p,t} \qquad \forall dra,p,w,t \qquad (6)$$

$$\sum_{\omega\in\Omega} \pi_\omega \sum_{t\in T^{On}_{dra,p,t}} F_{dra,p,\omega,t} \le E_{dra,p} \qquad \forall dra,p \qquad (7)$$

$$\sum_{t\in T^{On}_{dra,p,t}} I_{dra,p,t} \le N_{dra,p} \qquad \forall dra,p \qquad (8)$$

The first constraint limits the maximum capacity of DR program p by DRA dra at time t. Constraints (2) and (3) respectively declare the status of DR program p at time t, and the initializing and stopping states of the given DR program. Equations (4) and (5) consider the minimum and maximum duration of DR program p, respectively [23]. Constraint (6) imposes that load increase/decrease in two consecutive periods is limited by a maximum rate of change. The energy limit of the DR program is limited in constraint (7). Finally, the number of DR programs that can be carried out during a day is posed in (8). Note that we assume that the given DR program is OFF previous to time step 1.

The above formulation is a general representation of the following programs. Load shifting (ls) aims at moving the consumers' load from peak to off-peak periods. For example, a DR aggregator asks its residential consumers to avoid using their appliances such as washing machine or dishwasher during the peak period. The shifted load through load shifting programs has to be recovered in off-peak periods, which is carried out by load recovery (lrc) programs. These programs have received less attention in existing studies, where they are considered to have lump recovered load without any control. However, as mentioned earlier, proper management of load recovery programs could help better utilize (less spillage) wind and solar PV during off-peak. Equations (1)-(8) are used to model these programs, whereas load shifting aims at reducing the load through these equations while load recovery aims at increasing the load. In addition, constraint (9) is required to ensure that the load shifting volume is recovered through the load recovery program. Note that the recovery volume depends on the recovery factor ($RCF_{dra,ls}$) which is given by customers. Note also that subscriptions of ls and lrc describe load shifting and load recovery programs, as declared in the nomenclature.

$$\sum_{t\in T^{On}_{dra,ls,t}} F_{dra,ls,\omega,t} = RCF_{dra,ls} \sum_{t\in T^{On}_{dra,lrc,t}} F_{dra,lrc,\omega,t} \quad \forall dra,ls,lrc \tag{9}$$

Load curtailment (lc) has more flexibility than load shifting, though having the same aim. Those loads that can be curtailed without requiring recovery in off-peak periods can participate in this program. Here, equations (1)-(8) are valid for load curtailment programs. As for load growth (lg) programs, a DR aggregator aims to encourage consumers to increase their load, e.g. a factory to have more production. As discussed earlier, this program is particularly important when the ISO tries to avoid renewable energy spillage. load recovery and load growth programs aim at encouraging consumers to use more energy during specific periods. Here again equations (1)-(8) are valid, while load increment is the aim.

Note that the main reason behind including such constraints in the DR model is that the given constraints can avoid misleading the aggregator when making its DR offer in the market. Further, the DR aggregator requires providing its DR constraints to the market operator when bidding in the market in a similar way as for generators.

The DR model with the given constraints is realistic, which is used by DR aggregators and utilities worldwide [37-39].

Overall, load shifting (*ls*) and load curtailment (*lc*) are used when the DRA provides reserve up services in the market (see (10)), while load recovery (*lrc*) and load growth (*lg*) are applicable in reserve down offers by the DRA (11).

$$P^{\text{Dep,R-up}}_{dra,\omega,t} = \sum_{lc=1}^{LC} F_{dra,lc,\omega,t} + \sum_{ls=1}^{LS} F_{dra,ls,\omega,t} \quad \forall dra,\omega,t \tag{10}$$

$$P^{\text{Dep,R-dn}}_{dra,\omega,t} = \sum_{lrc=1}^{LRC} F_{dra,lrc,\omega,t} + \sum_{\text{lg}=1}^{LG} F_{dra,\text{lg},\omega,t} \quad \forall dra,\omega,t \tag{11}$$

B. Modeling the EV Aggregator

In this Section, the model of the EVA as an emerging player in electricity markets is presented. The behavior of EVAs is associated with the uncertain behavior of their customers. The behavior of EVs including the arrival and departure time of each EV, and its SOC at the arrival time are considered uncertain. According to the patterns of arrival/departure of electric vehicles, EVA charging/discharging is computed in the energy and reserve markets considering various technical and social constraints, given as follows.

Giving the charging/discharging rate of EV batteries, the maximum amounts of tradable power between each EVA and the grid are formulated in (12)-(14).

$$P^{\text{En,G2EVA}}_{eva,\omega,t} + P^{\text{Dep,R-dn}}_{eva,\omega,t} \le U^{\text{G2EVA}}_{eva,\omega,t} \sum_{n=1}^{N_{eva,\omega,t}} \gamma^{\text{ch}}_n \quad \forall eva,\omega,t \tag{12}$$

$$P^{\text{En,EVA2G}}_{eva,\omega,t} + P^{\text{Dep,R-up}}_{eva,\omega,t} \le U^{\text{EVA2G}}_{eva,\omega,t} \sum_{n=1}^{N_{eva,\omega,t}} \gamma^{\text{dch}}_n \quad \forall eva,\omega,t \tag{13}$$

$$U^{\text{G2EVA}}_{eva,\omega,t} + U^{\text{EVA2G}}_{eva,\omega,t} \le 1 \quad \forall eva,\omega,t \tag{14}$$

where

$$\begin{cases} P^{\text{En}}_{eva,\omega,t} = P^{\text{En,EVA2G}}_{eva,\omega,t} - P^{\text{En,G2EVA}}_{eva,\omega,t} \\ P^{\text{En,EVA2G}}_{eva,\omega,t} \ge 0 \\ P^{\text{En,G2EVA}}_{eva,\omega,t} \ge 0 \end{cases} \quad \forall eva,\omega,t \tag{15}$$

Inequality (12) ensures that the drawn power from the grid (from both energy and reserve down markets) is less than the charging rate of EVs. Similarly, expression (13) limits the injected power back to the grid to the discharging rate of EVs. Constraint (14) ensures the EVA charging/discharging status. Constraint (15) indicates the direction of the transferred power between the EVA and the grid. The positive value of $P^{\text{En}}_{eva,\omega,t}$ shows the injection of power from the EVA to the grid, while its negative value is defined as the power injection from the grid to the EVA.

The total State of Energy (SOE) of the EVA in each hour can be achieved from its stored energy in the previous hour plus the power traded with the grid and the SOE of plugged-in or unplugged vehicles, as formulated in (16) [27].

$$\begin{aligned} soe^{\text{EVA}}_{eva,\omega,t} &= soe^{\text{EVA}}_{eva,\omega,t-1} + soe^{\text{arv}}_{eva,\omega,t} - soe^{\text{dep}}_{eva,\omega,t} \\ &+ \left(P^{\text{En,G2EVA}}_{eva,\omega,t} + P^{\text{Dep,R-dn}}_{eva,\omega,t}\right)\eta^{\text{ch}}_{eva} - \frac{\left(P^{\text{En,EVA2G}}_{eva,\omega,t} + P^{\text{Dep,R-up}}_{eva,\omega,t}\right)}{\eta^{\text{dch}}_{eva}} \\ &\qquad \forall eva,\omega,t \end{aligned} \tag{16}$$

The SOE of arrived EVs can be calculated by the supposed scenario for an EVA's SOC as expressed in (17), whereas, the SOC of departed EVs is related to the supposed scenarios as well as the behavior of the EVA in charging/discharging EVs. The SOC is considered to be per unit. Therefore, the state of energy can be calculated by multiplying the capacity of EV by the SOC.

$$soe^{\text{arv}}_{eva,\omega,t} = \sum_{n=1}^{N_{eva,\omega,t}} Cap^{\text{EV}}_{n,\omega} soc^{\text{EV,ini}}_{n,\omega,t} \quad \forall eva,\omega,t \tag{17}$$

where $soe^{\text{arv}}_{eva,\omega,t}$ is the aggregated amount of stored energy that is added to the EVA, only because of new EVs' arrival.

The SOC of departed EVs also depends on the SOC of each departed EV as well as its battery capacity as presented in (18).

$$soe^{\text{dep}}_{eva,\omega,t} = \sum_{n=1}^{N_{eva,\omega,t}} Cap^{\text{EV}}_{n,\omega} soc^{\text{EV,dep}}_{n,\omega,t} \quad \forall eva,\omega,t \tag{18}$$

Eq. (19) denotes that the SOE of each EVA is equal to the summation of SOE of its EVs.

$$soe^{\text{EVA}}_{eva,\omega,t} = \sum_{n=1}^{N_{eva,\omega,t}} Cap^{\text{EV}}_{n,\omega} soc^{\text{EV}}_{n,\omega,t} \quad \forall eva,\omega,t \tag{19}$$

The SOC of each EV is also limited by inequality (20).

$$soc^{\min}_n \le soc^{\text{EV}}_{n,\omega,t} \le soc^{\max}_n \quad \forall n,\omega,t \tag{20}$$

EVAs have to charge each single EV to meet the desired SOC agreed with the EV owner. On this basis, an agreement between EVAs and their customers is assumed to ensure that the SOC of EVs at the departure time is greater than the desired amount, i.e., $soc^{\text{EV,ds}}_n$ (21).

This article has been accepted for publication in a future issue of this journal, but has not been fully edited. Content may change prior to final publication. Citation information: DOI 10.1109/TSG.2017.2777789, IEEE Transactions on Smart Grid

$$soc_{n,\omega,t}^{\text{EV,dep}} \geq soc_{n}^{\text{EV,ds}} \qquad \forall n,\omega,t \qquad (21)$$

The capacity of each EV depends on the EV battery class. The details of uncertainties of EVs are presented in Section III.

C. Market formulation

The ISO aims at minimizing the cost as in (22).

$$\begin{aligned}
\text{minimize}_{\Lambda} \\
&\sum_{t\in T}\sum_{i=1}^{NG}\left(C_{i,t}^{\text{SU}}+\lambda_{i,t}^{\text{En}}P_{i,t}^{\text{En}}+\lambda_{i,t}^{\text{Cap,R-up}}P_{i,t}^{\text{R-up}}+\lambda_{i,t}^{\text{Cap,R-dn}}P_{i,t}^{\text{R-dn}}\right)\\
&+\sum_{t\in T}\sum_{wpp\in WPP}\lambda_{wpp,t}^{\text{En}}P_{wpp,t}^{\text{En}}\\
&+\sum_{t\in T}\sum_{dra\in DRA}\left(\lambda_{dra,t}^{\text{Cap,R-up}}P_{dra,t}^{\text{R-up}}+\lambda_{dra,t}^{\text{Cap,R-dn}}P_{dra,t}^{\text{R-dn}}\right)\\
&+\sum_{t\in T}\sum_{eva\in EVA}\left(\lambda_{eva,t}^{\text{En}}P_{eva,t}^{\text{En}}+\lambda_{eva,t}^{\text{Cap,R-up}}P_{eva,t}^{\text{R-up}}+\lambda_{eva,t}^{\text{Cap,R-dn}}P_{eva,t}^{\text{R-dn}}\right)\\
&+\sum_{t\in T}\sum_{\omega\in\Omega}\pi_{\omega}\left[\begin{array}{l}
+\sum_{i\in 1}^{NG}\left(\lambda_{i,t}^{\text{R-up}}P_{i,\omega,t}^{\text{Dep,R-up}}-\lambda_{i,t}^{\text{R-dn}}P_{i,\omega,t}^{\text{Dep,R-dn}}\right)\\
+\sum_{dra\in DRA}\left(\lambda_{dra,t}^{\text{R-up}}P_{dra,\omega,t}^{\text{Dep,R-up}}-\lambda_{dra,t}^{\text{R-dn}}P_{dra,\omega,t}^{\text{Dep,R-dn}}\right)\\
+\sum_{eva\in EVA}\left(\lambda_{eva,t}^{\text{R-up}}P_{eva,\omega,t}^{\text{Dep,R-up}}-\lambda_{eva,t}^{\text{R-dn}}P_{eva,\omega,t}^{\text{Dep,R-dn}}\right)\\
\sum_{wpp\in WPP}C_{wpp}^{\text{sp}}P_{wpp,\omega,t}^{\text{sp}}+\sum_{j\in J}Voll_{j}L_{j,\omega,t}^{\text{Sh}}
\end{array}\right]
\end{aligned} \qquad (22)$$

The objective function is over the following variable set:

$$\Lambda=\{P_{i,t}^{\text{En}},P_{i,t}^{\text{R-up}},P_{i,t}^{\text{R-dn}},P_{wpp,t}^{\text{En}},P_{dra,t}^{\text{R-up}},P_{dra,t}^{\text{R-dn}},P_{eva,t}^{\text{En}},P_{eva,t}^{\text{R-up}},P_{eva,t}^{\text{R-dn}},P_{i,\omega,t}^{\text{Dep,R-up}},P_{i,\omega,t}^{\text{Dep,R-dn}},P_{dra,\omega,t}^{\text{Dep,R-up}},P_{dra,\omega,t}^{\text{Dep,R-dn}},P_{wpp,\omega,t}^{\text{sp}},L_{j,\omega,t}^{\text{Sh}}\}$$

The first line represents the cost of startup, energy and capacity reserves (upward and downward) by conventional generators. Line 2 indicates the costs related to wind power producers. The DR aggregator offers in the capacity market, with its capacity cost (upward and downward) formulated in line 3. Similar to conventional generators, it is assumed that EV aggregators offer in the energy and reserve markets. As such, the fourth line represents the cost of energy and capacity reserves by EVAs. The fifth to seventh lines represent the cost related to real-time market clearing, explained as follows. The costs (benefits) of upward (downward) reserve deployment from conventional generators, DRAs, and EVAs are given in lines five to seven, respectively. Finally, the last line provides the costs of wind spillage and involuntary load shedding.

The given problem is a two-stage stochastic programming approach, in which the first-stage decisions are independent of scenario realizations, and the second-stage decisions are dependent on scenario realizations.

1- Day-ahead constraints

The first-stage constraints are associated with the day-ahead electricity market, (23)-(36). DC power flow in the first-stage is given by (23).

Note that sunset (X_b) in the following equation indicate that the relevant generator, wind power producer, EV aggregator, load, and line(s) are connected to bus b. Note also that indices bs and br in equation (24) represent bus sending and receiving, respectively.

$$\begin{aligned}&\sum_{i\in I_n}P_{i,t}^{\text{En}}+\sum_{wpp\in WPP_b}P_{wpp,t}^{\text{En}}+\sum_{eva\in EVA_b}P_{eva,t}^{\text{En}}-\\&\sum_{j\in J_b}L_{j,t}^{\text{S}}-\sum_{l\in L_b}F_{l,t}=0 \qquad \forall b,t\end{aligned} \qquad (23)$$

$$F_{l,t}=(\delta_{bs,t}-\delta_{br,t})/X_l \qquad \forall l,t \qquad (24)$$

Transmission line flow limit is given by (25)

$$-F_l^{\max}\leq F_{l,t}\leq F_l^{\max} \qquad \forall l,t \qquad (25)$$

Power generation by wind power producer is constrained by its maximum capacity (determined by its capacity factor):

$$0\leq P_{wpp,t}^{\text{En}}\leq P_{wpp}^{\max} \qquad \forall wpp,t \qquad (26)$$

Power generation constraints of conventional generators:

$$P_{i,t}^{\text{En}}+P_{i,t}^{\text{R-up}}\leq P_i^{\max} \qquad \forall i,t \qquad (27)$$

$$P_{i,t}^{\text{En}}-P_{i,t}^{\text{R-dn}}\geq 0 \qquad \forall i,t \qquad (28)$$

Upward and downward reserve constraints are:

$$0\leq P_{i,t}^{\text{R-up}}\leq RU_i \qquad \forall i,t \qquad (29)$$

$$0\leq P_{i,t}^{\text{R-dn}}\leq RD_i \qquad \forall i,t \qquad (30)$$

Unit commitment constraints and variable declaration, as well as startup cost are represented by (31)-(34).

$$u_{i,t},I_{i,t},SD_{i,t}\in\{0,1\} \qquad \forall i,t \qquad (31)$$

$$u_{i,t}-u_{i,t-1}=I_{i,t}-SD_{i,t} \qquad \forall i,t \qquad (32)$$

$$I_{i,t}+SD_{i,t}\leq 1 \qquad \forall i,t \qquad (33)$$

$$C_{i,t}^{\text{SU}}\geq SUC_i(u_{i,t}-u_{i,t-1}) \qquad \forall i,t \qquad (34)$$

Up and down time constraints of generators are as follows.

$$(X_{i,t-1}^{\text{On}}-T_i^{\text{On}})(u_{i,t-1}-u_{i,t})\geq 0 \qquad \forall i,t \qquad (35)$$

$$(X_{i,t-1}^{\text{Off}}-T_i^{\text{Off}})(u_{i,t}-u_{i,t-1})\geq 0 \qquad \forall i,t \qquad (36)$$

2- Real-time constraints

The second-stage constraints are associated with actual system operation, (37)-(45).

Power balance at each bus for each time and scenario is given in (31) and (32).

$$\begin{aligned}&\sum_{i\in I_b}(P_{i,\omega,t}^{\text{Dep,R-up}}-P_{i,\omega,t}^{\text{Dep,R-dn}})+\sum_{wpp\in WPP_b}(P_{wpp,\omega,t}^{\text{Act}}-P_{wpp,t}^{\text{En}}-P_{wpp,\omega,t}^{\text{sp}})\\&+\sum_{eva\in EVA_b}(P_{eva,\omega,t}^{\text{Dep,R-up}}-P_{eva,\omega,t}^{\text{Dep,R-dn}})-\sum_{j\in J_b}(L_{j,\omega,t}^{\text{net}}-L_{j,t}^{\text{S}}-L_{j,\omega,t}^{\text{sh}})+\\&\sum_{dra\in DRA_b}(P_{dra,\omega,t}^{\text{Dep,R-up}}-P_{dra,\omega,t}^{\text{Dep,R-dn}})-\sum_{l\in L_b}F_{l,\omega,t}=0 \qquad \forall b,\omega,t\end{aligned} \qquad (37)$$

$$F_{l,\omega,t}=(\delta_{bs,\omega,t}-\delta_{br,\omega,t})/X_l \qquad \forall l,\omega,t \qquad (38)$$

This article has been accepted for publication in a future issue of this journal, but has not been fully edited. Content may change prior to final publication. Citation information: DOI 10.1109/TSG.2017.2777789, IEEE Transactions on Smart Grid

Transmission flow limit in real time for each scenario:

$$-F_l^{\max} \le F_{l,\omega,t} \le F_l^{\max} \qquad \forall l,\omega,t \tag{39}$$

Load shedding and wind spillage limits:

$$0 \le L_{j,\omega,t}^{\mathrm{sh}} \le L_{j,\omega,t}^{\mathrm{net}} \qquad \forall j,\omega,t \tag{40}$$

$$0 \le P_{wpp,\omega,t}^{\mathrm{sp}} \le P_{wpp,\omega,t}^{\mathrm{Act}} \qquad \forall wpp,\omega,t \tag{41}$$

The power output of generators in real time consists of their offers in energy and reserve markets:

$$P_{i,\omega,t}^{\mathrm{En}} = P_{i,t}^{\mathrm{En}} + P_{i,\omega,t}^{\mathrm{Dep,R\text{-}up}} - P_{i,\omega,t}^{\mathrm{Dep,R\text{-}dn}} \qquad \forall i,\omega,t \tag{42}$$

$$P_i^{\min} u_{i,t} \le P_{i,\omega,t}^{\mathrm{En}} \le P_i^{\max} u_{i,t} \qquad \forall i,\omega,t \tag{43}$$

Ramp rates of generators are constrained by (35)- (36).

$$P_{i,\omega,t}^{\mathrm{En}} - P_{i,\omega,t-1}^{\mathrm{En}} \le RU_i u_{i,t-1} + P_i^{\mathrm{SU}} I_{i,t} \qquad \forall i,\omega,t \tag{44}$$

$$P_{i,\omega,t-1} - P_{i,\omega,t} \le RD_i u_{i,t} + P_i^{\mathrm{SD}} SD_{i,t} \qquad \forall i,\omega,t \tag{45}$$

A- linking constraints

Constraints linking reserve deployment and reserve scheduled for generators and EVAs are shown in (46)-(47) and (48)-(49), respectively.

$$0 \le P_{i,\omega,t}^{\mathrm{Dep,R\text{-}up}} \le P_{i,t}^{\mathrm{R\text{-}up}} \qquad \forall i,\omega,t \tag{46}$$

$$0 \le P_{i,\omega,t}^{\mathrm{Dep,R\text{-}dn}} \le P_{i,t}^{\mathrm{R\text{-}dn}} \qquad \forall i,\omega,t \tag{47}$$

$$0 \le P_{eva,\omega,t}^{\mathrm{Dep,R\text{-}up}} \le P_{eva,t}^{\mathrm{R\text{-}up}} \qquad \forall eva,\omega,t \tag{48}$$

$$0 \le P_{eva,\omega,t}^{\mathrm{Dep,R\text{-}dn}} \le P_{eva,t}^{\mathrm{R\text{-}dn}} \qquad \forall eva,\omega,t \tag{49}$$

B- DR constraints

DR constraints for maximum reserve scheduling and reserve deployment are given in (50) and (54).

$$0 \le P_{dra,t}^{\mathrm{R\text{-}up}} \le RU_{dra}^{\mathrm{DR}} \qquad \forall dra,t \tag{50}$$

$$0 \le P_{dra,t}^{\mathrm{R\text{-}dn}} \le RD_{dra}^{\mathrm{DR}} \qquad \forall dra,t \tag{51}$$

$$0 \le P_{dra,\omega,t}^{\mathrm{Dep,R\text{-}up}} \le P_{dra,t}^{\mathrm{R\text{-}up}} \qquad \forall dra,\omega,t \tag{52}$$

$$0 \le P_{dra,\omega,t}^{\mathrm{Dep,R\text{-}dn}} \le P_{dra,t}^{\mathrm{R\text{-}dn}} \qquad \forall dra,\omega,t \tag{53}$$

Lastly, the constraints for various DR programs as well as that of EVAs given in Sections II-A and II-B are considered.

Equations (10)-(11) (54)

Equations (1)-(9) for LS and LRC (55)

Equations (1)-(8) for LC (56)

Equations (12)-(21) (57)

III. UNCERTAINTY CHARACTERIZATION

A. Probabilistic model of wind speed and solar

Wind power production depends on wind speed and wind turbines' characteristics. We use Weibull distribution function as a common function to model wind speed [40]. Using the probability distribution function of wind speed (PDFs), its scenarios are generated and then using the wind turbine power curve, they are transformed into wind power scenarios [32]. It should be noted that two different wind profiles (i.e., Wind 1 and Wind 2) are considered in this paper using their hourly historical data. In regard to solar PV, we used the historical data of solar power generation of the University of Queensland solar panels to generate our solar scenarios [32, 41].

B. Probabilistic model of EVs

In regard to EV scenarios, first, a capacity is set for each EV (n=1,…,N) by using the redundancy of the existing EV batteries as illustrated in Fig. 1 [42]. Then, in order to model the uncertainties of EVs' behavior, truncated Gaussian distribution is used for arrival and departure times and the SOC at arrival [31]. In order to generate the scenarios of EVs, the behavior of each EV is modeled using (58)-(60). Eq. (58) is used to generate scenarios for the arrival SOC of each EV.

$$soc_n^{\mathrm{EV,ini}} = f_{TG}\left(x;\mu_{soc};\ \sigma_{soc}^2;(soc_n^{\min};\ soc_n^{\max})\right) \qquad \forall n \tag{58}$$

where f_{TG} denotes the truncated Gaussian distribution. μ and σ^2 are mean value and variance of the random variable, respectively. Terms $(soc_n^{\min};soc_n^{\max})$ represent the truncation region. Similarly, (59) and (60) are used to generate the scenarios of arrival and departure times of each EV. According to (60), the departure time of each EV is a random variable $\in\left[\max\{t_n^{\mathrm{dep,min}},t_n^{\mathrm{arv}}+1\},t_n^{\mathrm{dep,max}}\right]$.

Therefore, terms $\max\{t_n^{\mathrm{dep,min}},t_n^{\mathrm{arv}}+1\}\le t_n^{\mathrm{dep}}$ and $t_n^{\mathrm{arv}}+1\le t_n^{\mathrm{dep}}$ guarantee that each EV arrives home before it leaves.

$$t_n^{\mathrm{arv}} = f_{TG}\left(x;\mu_{arv};\ \sigma_{arv}^2;(t_n^{\mathrm{arv,min}};\ t_n^{\mathrm{arv,max}})\right) \qquad \forall n \tag{59}$$

$$t_n^{\mathrm{dep}} = f_{TG}\left(x;\mu_{dep};\ \sigma_{dep}^2;(\max\{t_n^{\mathrm{dep,min}},t_n^{\mathrm{arv}}+1\};\ t_n^{\mathrm{dep,max}})\right) \tag{60}$$

Based on (58)-(60), different scenarios of SOC, arrival time and departure time are generated for N EVs (equal to 20,000 EVs for each EV aggregator), by using Roulette Wheel Mechanism (RWM) through truncated Gaussian distributions. The considered parameters of truncated Gaussian distributions are presented in Table I. Note that it is assumed that the behavior of each EV is independent of the other EV. Fig. 2 illustrates the Pseudo code for EV scenario generation.

C. System Characterization

It is assumed that the behavior of EVs is independent of weather conditions (i.e., PV and wind generation). Therefore, scenarios of EVs, as well as wind and PV are combined as three sets of independent scenarios.

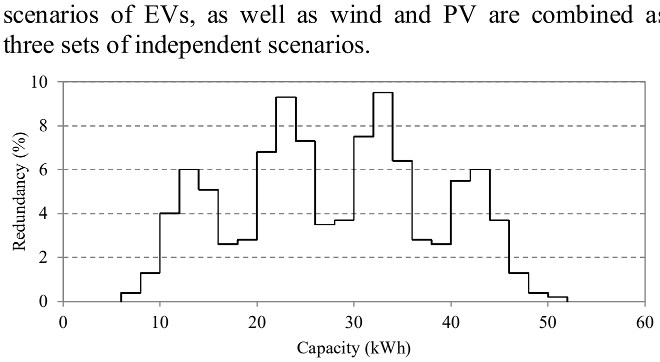

Fig. 1. Distribution of the battery capacity of EVs.

TABLE I
EVS PROBABILITY DISTRIBUTION

	Mean	Standard deviation	Min	Max
Initial EV SOE (%)	75	25	25	95
Arrival time (t^{arv})	19	2	16	24
Departure time (t^{dep})	7	2	5	12

Algorithm Scenario generation for EVs

for n=1 to N **do**

Assign a capacity (Cap_n^{EV}) to each EV by using the redundancy of EVs' batteries as presented in Fig. 1

Assign a minimum and a maximum SOC ($soc_n^{\text{EV,min}}$ and $soc_n^{\text{EV,max}}$) to each EV

end for

for ω=1 to Ω **do**

for n=1 to N **do**

Select a random SOC ($soc_n^{\text{EV,ini}}$) by using a Truncated Gaussian function Eq. (62)

Select a random arrival time (t_n^{arv}) by using a Truncated Gaussian function Eq. (63)

Select a random departure time (t_n^{dep}) by using a Truncated Gaussian function Eq. (64)

end for

Set $soc_{n,\omega,t}^{\text{EV,ini}} = soc_n^{\text{EV,ini}} \quad \text{if } t = t_n^{\text{arv}}$

end for

Fig. 2. The Pseudo code for EVs scenario generation

Therefore, N_s, $N_{wind\ 1}$ and $N_{wind\ 2}$ scenarios are generated for solar irradiance, wind speeds of Wind 1 and Wind 2, respectively. Note that each scenario process covers a 24-h time period of the typical day with its own probability of occurrence. A large number of scenarios may contribute to a more accurate model of the random variables. Nevertheless, it increases the computational burden of the problem. Thus, the scenarios are generated in such a way that they are small enough, but providing an approximation of random variable of the system.

IV. CASE STUDY

The modified single area IEEE reliability test system (24-bus system) and IEEE RTS-96 that is a multi-area reliability test system are used to indicate the performance of the proposed model. The latter is chosen due to its similarity to a large-scale power network containing a variety of generation.

All the case studies are formulated as mixed-integer programming and solved using CPLEX 11.1.1, GAMS [43].

A. The IEEE 24-bus system

The information of the 24-bus system is given in [44, 45]. Eleven DRAs are considered. The data for demand response programs are presented in [44]. The capacity and deployment costs of reserves up and down by generators are assumed 30% and 100% of their highest incremental cost of energy, respectively. Load recovery and load growth programs are considered for off-peak periods, which coincide peak rooftop PV and wind power generation. Load shifting and load curtailment, however, are assumed in the peak period. Ten wind farms are also modeled. Rooftop PV is assumed to be 20% of loads. The uncertainty of wind and PV power is considered using plausible scenarios as presented in [44]. The value of lost load (VOLL) is assumed $12000, and the cost of wind spillage is $100/MWh [45]. In addition, we assume that WPPs place their offer price at zero.

Four EVAs are considered at buses 4, 10, 16, and 20. Each EVA manages 20,000 EVs. As mentioned in Section II.B, the truncated Gaussian distribution is employed for arrival SOE, and arrival and departure times. In [31], the existing EV batteries are classified into twenty-four types. In this paper, it is assumed that each customer of the EVAs has one of these EV types. From each EVA's viewpoint, the redundancy of EV batteries is presented in [44]. The characteristics of each EV battery are presented in Table II. It is also assumed that each EV owner requires at least 90% of SOC at the departure time (i.e., $soc^{\text{EV,desired}} = 0.9$).

Six cases (C1-C6) are studied to investigate the interactions and behavior of the given multi-player model. Case 1 considers a power system integrating wind power only, while case 2 models the impact of rooftop PVs on the given power system and examines if this demand-side generation affects wind power generation. Case 3 studies the impact of DRAs on a market with uncertain wind power and rooftop PV, while no EVs are modeled in this case. Case 4, instead, examines the impact of uncontrolled EVs on the system while no DR is available. Case 5 is similar to case 4, but it models the interaction of DR and uncontrolled EVs in a renewable-integrated electricity market. Case 6 assesses how EVAs control the charging/discharging behavior of EVs and its impact on the given system.

In order to model the behavior of uncontrolled EVs, it is assumed that EV owners plug-in their EVs once they arrive home; hence, the EVs' battery starts charging at arrival time and keeps charging until the battery is fully charged. It is also assumed that the uncontrolled EVs are only operated in a gird-to-vehicle (G2V) mode. Therefore, EVs are modeled as loads that draw energy from the grid to be fully charged.

Wind power spillage for the given cases is depicted in Fig. 1. The results indicate that integrating rooftop PVs has a negligible impact on wind power spillage (see C1 vs. C2). This is mainly because roof-top PV generation is throughout the day that coincides with off-peak wind power production. Deploying DR in reserve markets (C3) leads to a considerable wind spillage reduction compared to case 2. While wind spillage volumes at hours 4 and 5 are almost negligible in case 3, that of hour 6 is just under 2 MWh. In case 4, where EVs are added to the system's load and no DR is used, wind spillage increases significantly and becomes almost equal to that of case 2. Wind spillage in case 5 that employs DR, however, falls to as low amount as case 3. Comparing C3-C5 clearly indicates that uncontrolled EVs have no impacts on wind spillage since EVs consumption in case 4 is mainly during off-peak wind power production. The interesting outcome is however, when aggregated EVs and DR are used in the system (i.e. C6), where the system does not spill wind power.

Figs. 3 and 4 present the reserves up and down provided by the DRA. The share of the DRA in reserve up follows a similar trend in all cases. The key findings are as follows. DR witnesses an overall increase when uncontrolled EVs are added to the system (see C3 vs. C5). This is particularly evident when EVs start to charge at 4 pm. The DRA increases its share of load reduction programs (i.e. load curtailment and load shifting) by around 25% in this hour. Further load reduction occurs at hours 6 pm and 8 pm. On the other hand, managing

This article has been accepted for publication in a future issue of this journal, but has not been fully edited. Content may change prior to final publication. Citation information: DOI 10.1109/TSG.2017.2777789, IEEE Transactions on Smart Grid

EVs by the EVA declines the overall share of the reserve up by the DRA, though there are some hours with more reserve-up by DR (see C6). It can be stated that the required reserve up by the system is distributed between the DRA and the EVA in such a way to reduce the system cost.

Fig. 5 illustrates that integrating uncontrolled EVs into the system has negligible impacts on downward reserve by DR. This was expected for uncontrolled EVs, where they do not inject power to the network. However, the results show that the aggregated EVs reduce the need for reserve down by the DRA, particularly in early morning. The reason behind this decline will be discussed in the following, when presenting the EVs' results. We further investigate the DRA's interaction in the market giving the share of each DR program in Figs. 6-9.

The share of load reduction programs, i.e. load curtailment and load shifting, is distributed in such a way that the load shifting program is mostly used in the first hours of the peak period, while the load curtailment program is used in the late evening. Further key interpretations are as follows. The amount of the load shifting program is much higher than the load curtailment program (see Table III). One reason could be the advantage of load shifting according to which the load can be recovered during off-peak periods. In particular, this advantage can be seen at hours 4-6 of the load recovery program (see Fig. 8), where this program is used to reduce wind spillage, as shown earlier in Fig. 3. Some interesting results can be interpreted in case 6, where load curtailment and load shifting tend to move to early afternoon and late evening, respectively. This changing pattern is justified by the discharging potential of the aggregated EVs, which will be discussed in following.

TABLE II
CONSIDERED DATA FOR EVs

$\eta_{eva}^{ch/dch}$	$\gamma_n^{ch/dch}$ (p.u./h)	soc_n^{min}	soc_n^{max}
0.9	0.2	0.2	1

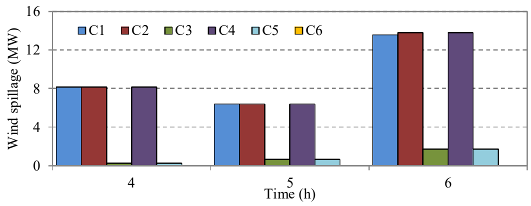

Fig. 3. Wind spillage in cases 1-6 to illustrate the impact of integration of wind, solar, DR, uncontrolled and aggregated EV.

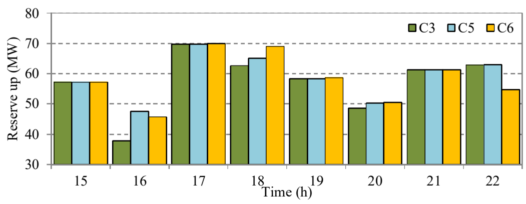

Fig. 4. Reserve up by the DRA in cases 3, 5 and 6 to illustrate the impact of interaction between DR and uncontrolled as well as aggregated EVs.

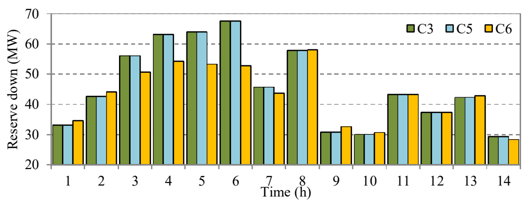

Fig. 5. Reserve down by the DRA DRA in cases 3, 5 and 6 to illustrate the impact of interaction between DR and uncontrolled as well as aggregated EVs.

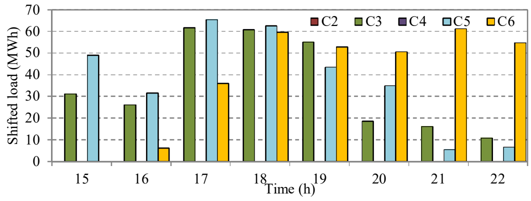

Fig. 6. Load shifting program, which indicates the impact of various renewables and EVs on the volume of this program.

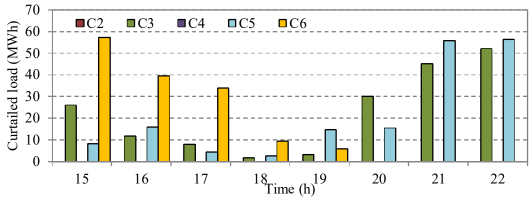

Fig. 7. Load curtailment program which indicates the impact of various renewables and EVs on the volume of this program.

TABLE III
LOAD SHIFTING AND LOAD CURTAILMENT IN DIFFERENT CASES (MWH)

	Load Curtailment	Load Shifting	Load Shifting	Load Growth
C3	178	280	280	363
C5	173.5	299	299	344.5
C6	146	321	321	286

The distributions of load recovery and load growth programs are provided in Figs. 8-9. While the load recovery program is used in the early morning to accommodate high production of wind power, the load growth program is useful during the day when rooftop PVs produce power. In addition, as a result of increasing the load shifting volume for the cases with EVs, the amount of the load recovery program also increases, especially at hours 5-10 am. On the other hand, the share of load growth declines, which is particularly evident in case 6. One reason is that the aggregated EVs need to charge in the midnight and accordingly, reduce the need for load growth (see Fig. 9).

Figs. 10 and 11 display charging and discharging patterns of aggregated electric vehicles. While the EVA procures their vehicles' energy from the reserve down market, they mostly use the energy market to discharge the vehicles. The EVA deploys energy from the reserve down market mostly in the early morning, which coincides with peak production of WPPs.

Compared to C4 and C5 that uncontrolled EVs are charged once they arrive at home, the aggregation of EVs can alleviate the severity of peak demand by shifting load to off-peak hours. The EVA manages to discharge vehicles during two periods.

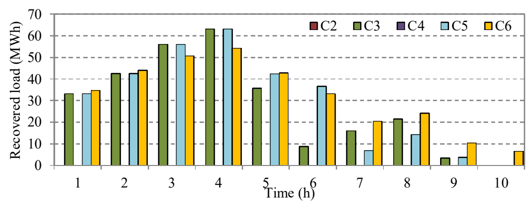

Fig. 8. Load recovery program which indicates the impact of various renewables and EVs on the volume of this program.

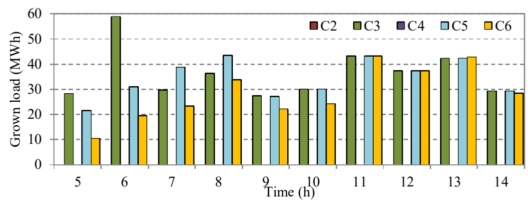

Fig. 9. Load growth program which indicates the impact of various renewables and EVs on the volume of this program.

This article has been accepted for publication in a future issue of this journal, but has not been fully edited. Content may change prior to final publication. Citation information: DOI 10.1109/TSG.2017.2777789, IEEE Transactions on Smart Grid

First, electric vehicles are partly discharged in the morning, where load is growing in the system. Then, the EVA discharges them in the evening, when vehicles arrive at home and the system is in its peak demand. This way, electric vehicles can alleviate the severity of peak demand with the hope of charging during the midnight. Note that the hours with both charging and discharging are related to different EVAs located on different buses. That is, while some EVs are charging in these hours, others are discharging.

Fig. 12 provides the expected cost of the system for the given cases. The highest system cost is for case 1, where there is only wind integrated to the system. This cost decreases to $345,000 when rooftop PVs are introduced in case 2, i.e. around 7% decrement compared to case 1. This is reasonable as rooftop PVs reduce the demand of the system, which accordingly leads to less generation requirement.

This decrement is even further when DR is employed by the ISO. In contrast, introducing electric vehicles without controlling their charging/discharging can significantly increase the system cost. This cost is even higher than case 2 where only renewable energy resources are integrated into the system. This indicates how destructive uncontrolled EVs would be for the future power systems. The adverse impact is more apparent when looking at case 5. This case illustrates that even using DR would not alleviate the high cost of uncontrolled EVs. Though the expected cost in case 5 declines compared to case 4, it is still just above case 2. Further, when observing case 6, which integrates DR and aggregated EVs, it is understood that controlling EVs reduces the cost by around 6%. The interesting point is when comparing system costs in cases 3 and 6, which indicates that introducing aggregated EVs in electricity markets would even decline the expected cost of the system.

The impact of different cases on LMPs is illustrated in Figs. 13 and 14. Fig. 13 indicates the hourly prices of bus 1 and bus 15 on the IEEE 24 bus system. Bus 1 is located on the lower side of the grid where the demand is higher than the generation and the voltage level is 138 kV, while Bus 15 is located on the upper side of the grid where the voltage level is 230 kV. By comparing the LMPs of case 2 and case 3 it can be observed that employing DR reduces the LMP in peak hours, while it increases the LMP in the valley hours. Moreover, by comparing cases 5 and 6 it can be seen that the aggregation of EVs has a significant impact on reducing the price in peak hours. EVAs also increase the price in the valley period. In periods 17 to 22, by employing EVAs the price decreases even more than the price in case 3 where EVs are not considered. This is due to the injected power by the aggregated EVs in the mentioned hours.

By comparing Figs. 13 and 14, it can be observed that the price at bus 15 is lower than bus 1. This is mainly due to the higher number of low cost generators in the upper side of the grid, while the capacity of the network avoids transferring the low cost power to the lower part of the network. For example, Fig. 15 indicates the expected loading of a transformer that is located between buses 3 and 24. As can be seen, the expected loading is higher than 85%. According to Fig. 15, case 6 has the highest impact on reducing the loading of the transformer in hours 17 to 21.

According to Figs, 13 and 14, it can be concluded that participation of DRAs and EVAs has a considerable impact on the prices of the areas where the network can restrict feeding by the low cost power. It should be noted that different prices and rewards of the emerging resources on different buses could significantly affect the loading of the network branches. The emerging resources can be allocated in a way to reduce the enhancement costs of the network.

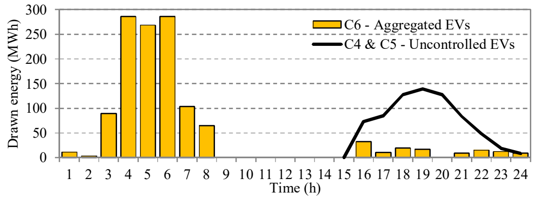

Fig. 10. Drawn energy by the vehicles from the grid, to compare the impact of uncontrolled and aggregated EVs.

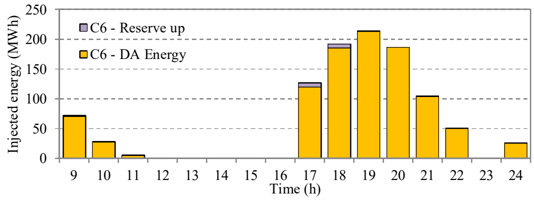

Fig. 11. Injected energy from the vehicles to the grid in the aggregated EV case.

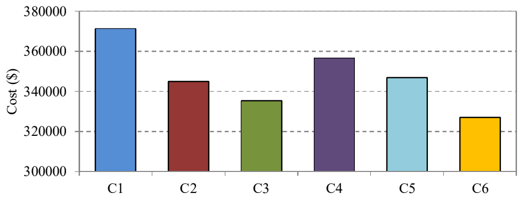

Fig. 12. The expected cost of the system in various cases.

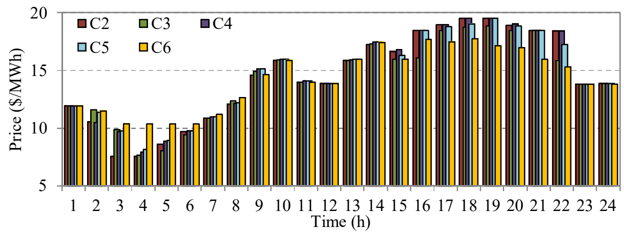

Fig. 13. Hourly price of bus 1 in different cases, to address the impact of wind, PV, DR, uncontrolled and aggregated EV on locational marginal prices.

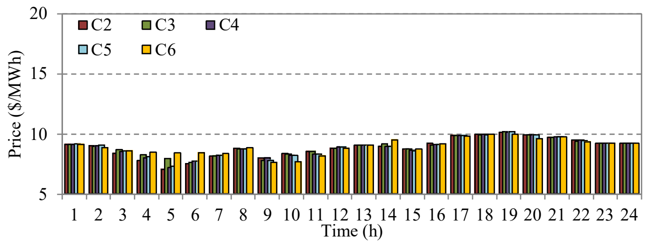

Fig. 14. Hourly price of bus 15 in different cases to address the impact of wind, PV, DR, uncontrolled and aggregated EV on locational marginal prices.

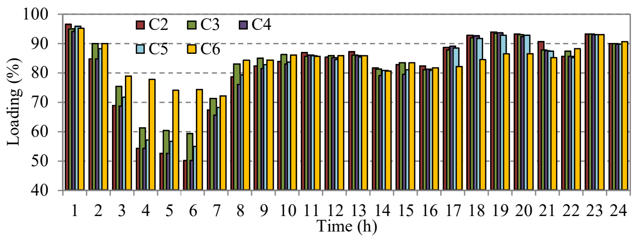

Fig. 15. Expected transformer loading in different cases to address the impact of wind, PV, DR, uncontrolled and aggregated EV on line loadings.

This article has been accepted for publication in a future issue of this journal, but has not been fully edited. Content may change prior to final publication. Citation information: DOI 10.1109/TSG.2017.2777789, IEEE Transactions on Smart Grid

B. The IEEE RTS three-area system

The modified IEEE RTS-96 is a three-area test system that is developed by linking various single 24-bus systems. It has 78 thermal units, 120 branches, 73 buses, and 51 load buses with 7950 MW daily peak load. Moreover, 30 wind farms, 35 DRAs, and 12 EVAs are added to the system in order to evaluate the effectiveness of the proposed model. Rooftop PV is assumed 20% of loads. Each EVA manages 20,000 EVs. The information of EVs is the same as the previous case study as presented in Tables I and II. Other assumptions are also the same as in the previous case study. Here, four cases are studied. Table IV indicates different cost terms of the system in various cases. It can be observed that EVs are more costly resources than DR to provide the capacity reserve. Moreover, DRAs can reduce the capacity reserve cost of generation companies better than EVAs. The DRAs are also more effective resources to reduce the wind spillage cost. Employing EVAs can reduce the total expected cost up to 4.2%. While DRAs are able to decrease the total expected cost by about 9.4%. In the last case where both DRAs and EVAs are employed, the total expected cost decreases by 12.2%. These results confirm findings from the 24-bus system, given earlier.

The traded power between the grid and the aggregators in the last case is illustrated in Figs. 16 and 17. Fig. 16 shows the expected drawn energy by DRAs and EVAs from the grid. It should be mentioned that the DRAs only participate in the reserve market, and the ISO prefers to operate the EVAs in the reserve down market rather than in the energy market to charge their EVs. Fig. 17 indicates the expected injected power from the DRAs and EVAs to the grid. EVAs operate in the energy market rather than in the reserve up market to inject their power back to the grid. These findings were also observed for the IEEE 24-bus system.

In order to indicate the applicability of the proposed model, the computation time and other optimization statistics of the model are reported in Tables V and VI. To this end, the computation time and the number of iterations are presented for four cases. The platform that has been used to evaluate the proposed model is a 64-bit Workstation with two Xeon E5-2687W 8C 3.10 GHz processors with 256 GB of RAM. Although the incorporation of DRAs and EVAs increases the computation time, this will not be a big problem for ISOs' using their high-speed workstations.

TABLE IV
TERMS OF COST OF THE IEEE RTS THREE-AREA SYSTEM

Case	w/o DRA w/o EVA	w/o DRA with EVA	with DRA w/o EVA	with DRA with EVA
Cost of Cap. Res. EVAs ($)	0	22864	0	19139
Cost of Dep. Res. EVAs ($)	0	-45627	0	-41815
Cost of energy EVAs ($)	0	36894	0	33850
Cost of Dep. Res. DRAs ($)	0	0	-40181	-40394
Cost of Dep. Res. Gencos	-132064	-118166	-101398	-93955
Cost of Cap. Res. DRAs ($)	0	0	14226	13775
Cost of Cap. Res. Gencos ($)	74551	69654	51676	48673
Cost of energy Gencos ($)	737018	703520	698698	679443
Wind spillage cost ($)	10101	5608	2171	1030
Expected cost ($)	693751	664374	628255	609456

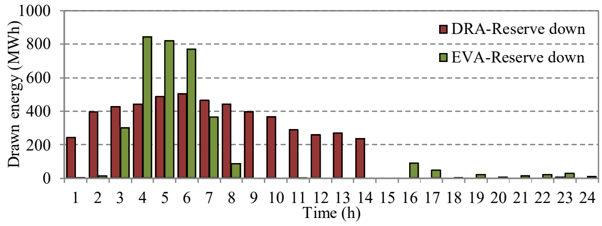

Fig. 16. Drawn energy by the EVAs and DRAs from the grid in case 6.

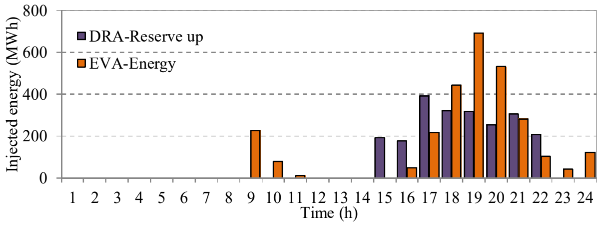

Fig. 17. Injected energy from the EVAs and DRAs to the grid in case 6.

TABLE V
COMPUTATION TIME FOR CASE STUDIES

Case	w/o DRA w/o EVA	w/o DRA with EVA	with DRA w/o EVA	with DRA with EVA
No. of iterations	61,038	145,165	86,181	172,793
Solution time (s)	38.8	491.9	91.1	814.6

TABLE VI
OPTIMIZATION STATISTICS OF THE PROPOSED MODEL

Blocks of equations	Single equations	Blocks of variables	Single variables	Non-zero elements	Discrete variables
113	358,497	73	165,610	1,230,813	13,248

V. CONCLUSIONS

This paper proposes a comprehensive market model to integrate practical constraints and behavior of the emerging resources in power systems. The given model formulates each emerging resource through unique mathematical formulation and then integrates them into electricity markets to investigate their impacts on each other and also market outcomes. The key findings are as follows.

1- DR and EV aggregators' participation in the energy and reserve markets considerably reduce the cost of the system. LMPs reduce during the peak period and increase during valley period. Further, wise employment of these aggregators in the market would help the loading of network branches and bring long-term benefits. It can thus not only help to reduce the LMPs in high cost part of the system but also to postpone the need for network enhancement and construction of new bulk facilities.

2- DR aggregators would help the ISO reduce wind spillage. While rooftop PVs have a negligible impact on the wind spillage reduction, uncontrolled EVs, however, can increase the peak load but without a positive effect in increasing wind spillage considerably. This is mainly due to the different time of energy production of wind energy. On the other hand, considering EV constraints in the developed EV aggregator model would further contribute to reducing wind spillage.

3- Modeling DR and EV constraints and behavior would help the ISO better utilize these resources. The ISO distributes the share of DRs and EVs with the aim of reducing the cost of the system. This is carried out according to the offers and constraints provided by their aggregators and to customers' limits and behavior as the proposed model satisfies both the power system and customers' requirements.

REFERENCES

[1] S. S. Reddy, P. R. Bijwe, and A. R. Abhyankar, "Joint Energy and Spinning Reserve Market Clearing Incorporating Wind Power and Load Forecast Uncertainties," *Systems Journal, IEEE,* vol. 9, no. 1, pp. 152-164, 2015.

[2] A. Botterud *et al.*, "Wind Power Trading Under Uncertainty in LMP Markets," *IEEE Transactions on Power Systems,* vol. 27, no. 2, pp. 894-903, 2012.

[3] C. Sun, Z. Bie, M. Xie, and G. Ning, "Effects of wind speed probabilistic and possibilistic uncertainties on generation system adequacy," *IET Generation, Transmission & Distribution,* vol. 9, no. 4, pp. 339-347, 2015.

[4] N. Mahmoudi, T. K. Saha, and M. Eghbal, "Demand Response Application by Strategic Wind Power Producers," *IEEE Transactions on Power Systems,* vol. 31, no. 2, pp. 1227-1237, 2016.

[5] M. J. E. Alam, K. M. Muttaqi, and D. Sutanto, "Mitigation of Rooftop Solar PV Impacts and Evening Peak Support by Managing Available Capacity of Distributed Energy Storage Systems," *Power Systems, IEEE Transactions on,* vol. 28, no. 4, pp. 3874-3884, 2013.

[6] H. Beltran, E. Perez, N. Aparicio, and P. Rodriguez, "Daily Solar Energy Estimation for Minimizing Energy Storage Requirements in PV Power Plants," *Sustainable Energy, IEEE Transactions on,* vol. 4, no. 2, pp. 474-481, 2013.

[7] (2015). *AEMO*. [Online] Available: http://www.aemo.com.au/

[8] J. M. Morales, A. J. Conejo, L. Kai, and Z. Jin, "Pricing Electricity in Pools With Wind Producers," *Power Systems, IEEE Transactions on,* vol. 27, no. 3, pp. 1366-1376, 2012.

[9] H. Nosair and F. Bouffard, "Economic Dispatch Under Uncertainty: The Probabilistic Envelopes Approach," *IEEE Transactions on Power Systems,* vol. PP, no. 99, pp. 1-1, 2016.

[10] G. L. Ray, E. M. Larsen, and P. Pinson, "Evaluating price-based demand response in practice - with application to the EcoGrid EU Experiment," *IEEE Transactions on Smart Grid,* vol. PP, no. 99, pp. 1-1, 2016.

[11] J. Brooks *et al.*, "An experimental investigation of occupancy-based energy-efficient control of commercial building indoor climate," in *53rd IEEE Conference on Decision and Control*, 2014, pp. 5680-5685.

[12] C. H. Wai, M. Beaudin, H. Zareipour, A. Schellenberg, and N. Lu, "Cooling Devices in Demand Response: A Comparison of Control Methods," *IEEE Transactions on Smart Grid,* vol. 6, no. 1, pp. 249-260, 2015.

[13] N. H. Tran, C. T. Do, S. Ren, Z. Han, and C. S. Hong, "Incentive Mechanisms for Economic and Emergency Demand Responses of Colocation Datacenters," *IEEE Journal on Selected Areas in Communications,* vol. 33, no. 12, pp. 2892-2905, 2015.

[14] D. T. Nguyen, H. T. Nguyen, and L. B. Le, "Dynamic Pricing Design for Demand Response Integration in Power Distribution Networks," *IEEE Transactions on Power Systems,* vol. 31, no. 5, pp. 3457-3472, 2016.

[15] P. Siano, "Demand response and smart grids—A survey," *Renewable and Sustainable Energy Reviews,* vol. 30, pp. 461-478, 2// 2014.

[16] M. Parvania and M. Fotuhi-Firuzabad, "Demand Response Scheduling by Stochastic SCUC," *Smart Grid, IEEE Transactions on,* vol. 1, no. 1, pp. 89-98, 2010.

[17] J. Aghaei and M. I. Alizadeh, "Robust n-1 contingency constrained unit commitment with ancillary service demand response program," *Generation, Transmission & Distribution, IET,* vol. 8, no. 12, pp. 1928-1936, 2014.

[18] D. T. Nguyen and L. B. Le, "Risk-Constrained Profit Maximization for Microgrid Aggregators With Demand Response," *IEEE Transactions on Smart Grid,* vol. 6, no. 1, pp. 135-146, 2015.

[19] P. Siano and D. Sarno, "Assessing the benefits of residential demand response in a real time distribution energy market," *Applied Energy,* vol. 161, pp. 533-551, 1/1/ 2016.

[20] S. Gottwalt, J. Gärttner, H. Schmeck, and C. Weinhardt, "Modeling and Valuation of Residential Demand Flexibility for Renewable Energy Integration," *IEEE Transactions on Smart Grid,* vol. PP, no. 99, pp. 1-10, 2016.

[21] J. Knudsen, J. Hansen, and A. M. Annaswamy, "A Dynamic Market Mechanism for the Integration of Renewables and Demand Response," *IEEE Transactions on Control Systems Technology,* vol. 24, no. 3, pp. 940-955, 2016.

[22] N. Gatsis and G. B. Giannakis, "Decomposition Algorithms for Market Clearing With Large-Scale Demand Response," *Smart Grid, IEEE Transactions on,* vol. PP, no. 99, pp. 1-12, 2013.

[23] M. Parvania, M. Fotuhi-Firuzabad, and M. Shahidehpour, "ISO's Optimal Strategies for Scheduling the Hourly Demand Response in Day-Ahead Markets," *Power Systems, IEEE Transactions on,* vol. 29, no. 6, pp. 2636-2645, 2014.

[24] F. Rassaei, W. S. Soh, and K. C. Chua, "Demand Response for Residential Electric Vehicles With Random Usage Patterns in Smart Grids," *IEEE Transactions on Sustainable Energy,* vol. 6, no. 4, pp. 1367-1376, 2015.

[25] X. Bai and W. Qiao, "Robust Optimization for Bidirectional Dispatch Coordination of Large-Scale V2G," *IEEE Transactions on Smart Grid,* vol. 6, no. 4, pp. 1944-1954, 2015.

[26] W. Qi, Z. Xu, Z. J. M. Shen, Z. Hu, and Y. Song, "Hierarchical Coordinated Control of Plug-in Electric Vehicles Charging in Multifamily Dwellings," *IEEE Transactions on Smart Grid,* vol. 5, no. 3, pp. 1465-1474, 2014.

[27] N. Neyestani, M. Y. Damavandi, M. Shafie-khah, A. Bakirtzis, and J. P. S. Catalao, "Plug-in Electric Vehicles Parking Lot Equilibria with Energy and Reserve Markets," *IEEE Transactions on Power Systems,* vol. PP, no. 99, pp. 1-1, 2016.

[28] Z. Chaoyue, W. Jianhui, J. P. Watson, and G. Yongpei, "Multi-Stage Robust Unit Commitment Considering Wind and Demand Response Uncertainties," *Power Systems, IEEE Transactions on,* vol. 28, no. 3, pp. 2708-2717, 2013.

[29] M. E. Khodayar, L. Wu, and M. Shahidehpour, "Hourly Coordination of Electric Vehicle Operation and Volatile Wind Power Generation in SCUC," *IEEE Transactions on Smart Grid,* vol. 3, no. 3, pp. 1271-1279, 2012.

[30] H. N. T. Nguyen, C. Zhang, and M. A. Mahmud, "Optimal Coordination of G2V and V2G to Support Power Grids With High Penetration of Renewable Energy," *IEEE Transactions on Transportation Electrification,* vol. 1, no. 2, pp. 188-195, 2015.

[31] S. I. Vagropoulos and A. G. Bakirtzis, "Optimal Bidding Strategy for Electric Vehicle Aggregators in Electricity Markets," *IEEE Transactions on Power Systems,* vol. 28, no. 4, pp. 4031-4041, 2013.

[32] N. Mahmoudi, M. Shafie-khah, T. K. Saha, and J. P. S. Catalão, "Customer-driven demand response model for facilitating roof-top PV and wind power integration," *IET Renewable Power Generation*, vol. 11, no. 9, pp. 1200-1210, 2017.

[33] N. Aparicio, I. MacGill, J. Rivier Abbad, and H. Beltran, "Comparison of Wind Energy Support Policy and Electricity Market Design in Europe, the United States, and Australia," *Sustainable Energy, IEEE Transactions on,* vol. 3, no. 4, pp. 809-818, 2012.

[34] AEMO, "100 PER CENT RENEWABLES STUDY –MODELLING OUTCOMES," 2013, [Online] Available: https://www.environment.gov.au/system/files/resources/d67797b7-d563-427f-84eb-c3bb69e34073/files/100-percent-renewables-study-modelling-outcomes-report.pdf.

[35] S. A. N. Toby Brown, David Luke Oates, Kathleen Spees, "International Review of Demand Response Mechanisms," 2015, [Online] Available: http://www.brattle.com/system/publications/pdfs/000/005/220/original/AEMC_Report.pdf?1448478639.

[36] R. J. Bessa, M. A. Matos, F. J. Soares, and J. A. P. Lopes, "Optimized Bidding of a EV Aggregation Agent in the Electricity Market," *IEEE Transactions on Smart Grid,* vol. 3, no. 1, pp. 443-452, 2012.

[37] P. G. a. E. Company. (2016). *SmartAC program*. [Online] Available: http://www.pge.com/en/mybusiness/save/energymanagement/smartac/index.page

[38] ENERGEX. (2016). *PeakSmart air-conditioning*. [Online] Available: https://www.energex.com.au/residential-and-business/positive-payback/positive-payback-for-households/households

[39] ENERNOC. (2016). *Demand Response Resources to Southern California Edison*. [Online] Available: https://www.enernoc.com/resources/case-studies/southern-california-edison-company

[40] Y. M. Atwa, E. F. El-Saadany, M. M. A. Salama, and R. Seethapathy, "Optimal Renewable Resources Mix for Distribution System Energy Loss Minimization," *Power Systems, IEEE Transactions on,* vol. 25, no. 1, pp. 360-370, 2010.

[41] U. Queensland. (2016). *UQ Solar*. [Online] Available: http://solar.uq.edu.au/user/reportPower.php

[42] Y. K. Jemal, "Plug-in electric vehicle charging impacts on power systems," Master Degree, Chalmers Univ. of Tech., Chalmers Univ. of Tech., Goteborg, Sweden, 2010.

[43] *GAMS Website*. [Online] Available: http://www-01.ibm.com/software/integration/optimization/cplex-optimizer-zos/

[44] N. Mahmoudi. M. Shafie-khah, P. Siano, and T.K. Saha, "A modified 24-bus system including wind farms, roof-top PVs, demand response and electric vehicles," ed, 2016, doi: 10.13140/RG.2.1.2656.2169.

[45] A. J. Conejo, M. Carrión, and J. M. Morales, *Decision Making Under Uncertainty in Electricity Markets*. Springer US, 2010.

This article has been accepted for publication in a future issue of this journal, but has not been fully edited. Content may change prior to final publication. Citation information: DOI 10.1109/TSG.2017.2777789, IEEE Transactions on Smart Grid

BIOGRAPHIES

Miadreza Shafie-khah (M'13-SM'17) received the M.Sc. and Ph.D. degrees in electrical engineering from Tarbiat Modares University, Tehran, Iran, in 2008 and 2012, respectively. He received his first postdoc from the University of Beira Interior (UBI), Covilha, Portugal in 2015, while working on the 5.2-million-euro FP7 project SiNGULAR ("Smart and Sustainable Insular Electricity Grids Under Large-Scale Renewable Integration"). He received his second postdoc from the University of Salerno, Salerno, Italy in 2016. He is currently an Invited Assistant Professor and Senior Researcher at C-MAST/UBI, where he has a major role of co-coordinating a WP in the 2.1-million-euro national project ESGRIDS ("Enhancing Smart GRIDS for Sustainability"), while co-supervising four PhD students and two post-doctoral fellows. He was considered one of the Outstanding Reviewers of IEEE TSTE, in 2014, and one of the IEEE TSG Best Reviewers in 2016. His research interests include power market simulation, market power monitoring, power system optimization, demand response, electric vehicles, price forecasting and smart grids.

Nadali Mahmoudi (S'08–M'15) received the B.Sc. in electrical engineering from Isfahan University of Technology, Iran, in 2007, the M.Sc. degree in power engineering from Tarbiat Modares University, Tehran, Iran, in 2010, and the Ph.D. degree in electrical power engineering from the University of Queensland, Brisbane, Australia, in 2015. He received his Postdoc at the School of Information Technology and Electrical Engineering, University of Queensland, in 2017. His research interests include demand response, electricity markets, renewable energy, optimization and stochastic programming.

Pierluigi Siano (M'09-SM'14) received the M.Sc. degree in electronic engineering and the Ph.D. degree in information and electrical engineering from the University of Salerno, Salerno, Italy, in 2001 and 2006, respectively. He is an Associate Professor of electrical energy engineering with the Department of Industrial Engineering University of Salerno. He has coauthored more than 300 papers including more than 150 international journal papers. His research interests include the integration of distributed energy resources in smart distribution systems and planning and management of power systems. Dr. Siano is the Chair of the Technical Committee on Smart Grids and a member of the Technical Committee on Renewable Energy Systems of the IEEE INDUSTRIAL ELECTRONICS SOCIETY. He is an Editor of Intelligent Industrial Systems (Springer), an Associate Editor of the IEEE TRANSACTIONS ON INDUSTRIAL INFORMATICS, and a member of the Editorial Board of more than 30 International Journals.

Tapan K. Saha (SM'97) was born in Bangladesh and immigrated to Australia in 1989. Currently, he is a Professor of electrical engineering in the School of Information Technology and Electrical Engineering, University of Queensland, Brisbane, Australia. Before joining the University of Queensland in 1996, he taught at the Bangladesh University of Engineering and Technology, Dhaka, for three and a half years and then at James Cook University, Townsville, Australia, for two and a half years. His research interests include power systems, power quality, and condition monitoring of electrical plants. Prof. Saha is a Fellow of the Institution of Engineers, Australia.

João P. S. Catalão (M'04-SM'12) received the M.Sc. degree from the Instituto Superior Técnico (IST), Lisbon, Portugal, in 2003, and the Ph.D. degree and Habilitation for Full Professor ("Agregação") from the University of Beira Interior (UBI), Covilha, Portugal, in 2007 and 2013, respectively.

Currently, he is a Professor at the Faculty of Engineering of the University of Porto (FEUP), Porto, Portugal, and Researcher at INESC TEC, INESC-ID/IST-UL, and C-MAST/UBI. He was the Primary Coordinator of the EU-funded FP7 project SiNGULAR ("Smart and Sustainable Insular Electricity Grids Under Large-Scale Renewable Integration"), a 5.2-million-euro project involving 11 industry partners. He has authored or coauthored more than 575 publications, including 200 journal papers (more than 50 IEEE Transactions/Journal papers), 330 conference proceedings papers, 31 book chapters, and 14 technical reports, with an *h*-index of 34, an *i10*-index of 123, and over 5100 citations (according to Google Scholar), having supervised more than 50 post-docs, Ph.D. and M.Sc. students. He is the Editor of the books entitled *Electric Power Systems: Advanced Forecasting Techniques and Optimal Generation Scheduling* and *Smart and Sustainable Power Systems: Operations, Planning and Economics of Insular Electricity Grids* (Boca Raton, FL, USA: CRC Press, 2012 and 2015, respectively). His research interests include power system operations and planning, hydro and thermal scheduling, wind and price forecasting, distributed renewable generation, demand response and smart grids.

Prof. Catalão is an Editor of the IEEE TRANSACTIONS ON SMART GRID, an Editor of the IEEE TRANSACTIONS ON SUSTAINABLE ENERGY, an Editor of the IEEE TRANSACTIONS ON POWER SYSTEMS, and an Associate Editor of the *IET Renewable Power Generation*. He was the Guest Editor-in-Chief for the Special Section on "Real-Time Demand Response" of the IEEE TRANSACTIONS ON SMART GRID, published in December 2012, and the Guest Editor-in-Chief for the Special Section on "Reserve and Flexibility for Handling Variability and Uncertainty of Renewable Generation" of the IEEE TRANSACTIONS ON SUSTAINABLE ENERGY, published in April 2016. Since May 2017, he is the Corresponding Guest Editor for the Special Section on "Industrial and Commercial Demand Response" of the IEEE TRANSACTIONS ON INDUSTRIAL INFORMATICS. He was the recipient of the 2011 Scientific Merit Award UBI-FE/Santander Universities and the 2012 Scientific Award UTL/Santander Totta, in addition to an Honorable Mention in the 2017 Scientific Awards ULisboa/Santander Universities. Moreover, he has won 4 Best Paper Awards at IEEE Conferences.